Article

Optimization of Ultrasonic-Assisted Extraction by Response Surface Methodology with Maximal Phenolic Yield and Antioxidant Activity from *Acer truncatum* Leaves

Lingguang Yang †, Peipei Yin †, Hang Fan, Qiang Xue, Ke Li, Xiang Li, Liwei Sun* and Yujun Liu *

National Engineering Laboratory for Tree Breeding, College of Biological Sciences and Biotechnology, Beijing Forestry University, Beijing 100083, China; yanglingguangxdjqz@163.com (L.Y.); happy62889@126.com (P.Y.); fwqh1990@163.com (H.F.); like17931@163.com (K.L.); 18289743335@163.com (X.L.)

* Correspondence: lsun2013@bjfu.edu.cn (L.S.); yjliubio@bjfu.edu.cn (Y.L.); Tel.: +86-13691397366 (L.S.); +86-13521148866 (Y.L.)

† These authors equally made contributions to this article, and thus should be considered as co-first authors.

Abstract: This study was designed for the first time to improve phenolic yield and antioxidant activity of ultrasonic-assisted extraction from *Acer truncatum* leaves (ATL) using response surface methodology, and phenolic composition in ATL extracted under the optimized condition were characterized by UPLC-QTOF-MS/MS. Solvent and extraction time were selected based on preliminary experiments, and a four-factors-three-levels central composite design was conducted to optimize solvent concentration (X_1), material-to-liquid ratio (X_2), ultrasonic temperature (X_3) and power (X_4) for an optimal total phenol yield (Y_1) and DPPH• antioxidant activity (Y_2). The results showed that the optimal combination was ethanol: water (v:v) 66.21%, material-to-liquid ratio 1:15.31 g/mL, ultrasonic temperature 60 °C, power 267.30 W, and time 30 min with three extractions, giving a maximal total phenol yield of 7593.62 mg gallic acid equivalent /100 g d.w. and a maximal DPPH• antioxidant activity of 74241.61 µmol Trolox equivalent/100 g d.w.. Furthermore, 22 phenolics were first identified in ATL extract obtained under the optimized conditions, indicating that gallates, gallotannins, quercetin, myricetin and chlorogenic acid derivatives were the main phenolic composition in ATL. What's more, a gallotannins pathway existing in ATL from gallic acid to penta-*O*-galloyl-glucoside was interpreted. All these results provided practical information aiming at full utilization of phenolics in ATL, together with fundamental knowledge for further research.

Keywords: *Acer truncatum* leaves; ultrasonic-assisted extraction; response surface methodology; phenolics; antioxidant activity; UPLC-QTOF-MS/MS

1. Introduction

Acer truncatum is a prominent maple (*Aceraceae*) species widely cultivated in China, Korea and Japan, and is also found in Europe and Northern America [1,2]. In northern China, maple leaves, mainly *A. truncatum* leaves (ATL), are often used as healthy drinks and folk medicines treating coronary artery cirrhosis, cerebrovascular diseases and angina pectoris [3]. Previous investigations of ATL indicated that it possessed various biological functions, such as antioxidant [4], antibacterial [5,6], and antitumor [7,8] due to its high contents of tannins, flavonoids, and chlorogenic acid. However, little effort has been made to the optimization of extraction method of phenolics in ATL. Therefore, in order to ensure the full utilization of ATL, an ultrasound-assisted extraction (UAE) method was established through response surface methodology (RSM) in the current study.

UAE is well recognized to exhibit positive effects on the rate of various extraction processes in food, pharmaceutical and cosmetic industries. Comparing to other conventional methods, UAE offers a net advantage in terms of productivity and selectivity with shorter processing time, enhanced quality, reduced chemical and physical hazards, and it is environmentally friendly and causes less damage to the structural and molecular properties of compounds in plant materials [9,10]. For these reasons, UAE from plant materials has been widely used lately to facilitate extractions of phenols from *Chrysanthemum morifolium* flower head [10], *Olea europaea* fruit [11], *Morus nigra* must [12], and *Curcuma longa* rhizome [13], lipids from rice [14], polysaccharides from pumpkin [15] and mycelial fermentation of *Phellinus igniarius* [16], proteins from *Jatropha curcas* seed [17], lignans from *Schisandra chinensis* fruit [18] and other value-added compounds from various natural resources. However, to the best of our knowledge, no effort is available regarding improvements of phenolic yield by itself, let alone the phenolic yield together with antioxidant activity from ATL by ultrasonic stimulation. Thus the present study could provide economic information for the industrial manufacture of ATL as phenolic and antioxidant resource. Nevertheless, the extraction yield of chemical constituents from crude plant materials was affected by many factors. When utilizing an UAE method, factors such as extraction solvent, extraction time, material-to-liquid ratio, ultrasound power and extraction temperature were generally considered to have significant effects on the extraction efficiency. Therefore, when a new UAE method for ATL is developed, optimization of these extraction conditions is indispensable for the best extraction effect.

Being a valuable tool to investigate the interaction among factors and quantitatively depict the effects of given parameters on their measured responses [19], RSM is a collection of statistical and mathematical methods for developing, improving, and optimizing a process [20]. In comparison with single variable optimization methods, RSM is a time- and cost-effective means of simultaneously evaluating interactions as well as the key experimental parameters [21], thus have been wildly applied to optimize many bioprocesses [17,22-24]. Central composite design (CCD) used in RSM, is more superior comparing with the classical approach in terms of the comprehensiveness of information gained and the accuracy of the experiment conducted [22,25], thus is applied in the present study to optimize the UAE process.

LC-MS/MS technique is gaining increasing interest in the characterization of phenolic compositions due to its high selectivity and sensitivity [26-28]. For example, Melguizo-Melguizo et al. [29] analyzed 22 compounds from *Artemisia vulgaris* leaves, 15 of them were phenolics; and Kolniak-Ostek [30] tentatively identified 65 phenolic components in ten pear cultivars. Therefore, the variety of phenolics in ATL extract, determined with UPLC-QTOF-MS/MS analysis under the optimized extraction condition, was analyzed to investigate the phenolic composition as well as the quality of the extraction.

Overall, the present study was designed to optimize the UAE process with RSM and CCD for the maximum phenolic yield and antioxidant activity from ATL. And phenolic composition of the ATL extract obtained under the optimized UAE condition was analyzed with the UPLC-QTOF-MS/MS technique. These results would contribute to the base-line data for industrial manufacture as well as further exploitation of ATL as a phenolic and antioxidant resource.

2. Results and Discussion

2.1. Effects of solvents and independent variables on UAE

2.1.1. Solvent types

Phenolic yield obtained with different extraction solvent [water, methanol, ethanol, methanol: water (1:1, v:v), or ethanol : water (1:1, v:v)] was firstly determined to select the best solvent (combination). Results show that different solvents significantly affected phenolic yield (Figure 1A). The phenolic yield with methanol (5112.17 GAE/100 g d.w.) was slightly higher than that with ethanol (5049.23), and both of them were significantly higher than that with water (602.63). However, when ethanol was combined with water at the ratio of 1:1 (v:v), phenols extracted was significantly increased to 7262.61. This result was consistent with several previous studies that aqueous organic solvents exhibit a higher extraction efficiency than absolute organic solvents [33-35]. Cujic et al. [36]

Preprints (www.preprints.org) | NOT PEER-REVIEWED | Posted: 9 January 2017 doi:10.20944/preprints201701.0036.v1

Peer-reviewed version available at Molecules 2017, 22, 232; doi:10.3390/molecules22020232

explained this phenomenon as water takes response for swelling of plant material while ethanol is responsible for disrupting the bonding between the solutes and plant matrix, and just this synergistic effect leads to a higher phenolic yield. However, phenolic yield with methanol: water (1:1, v:v) exhibited a worse result (2369.13) comparing with that extracted merely with methanol. It might resulted from its unappropriated polarity for extraction targeting phenols in ATL. Therefore, ethanol but not methanol, and aqueous ethanol, instead of pure ethanol, was selected as the best solvent for phenolic extraction.

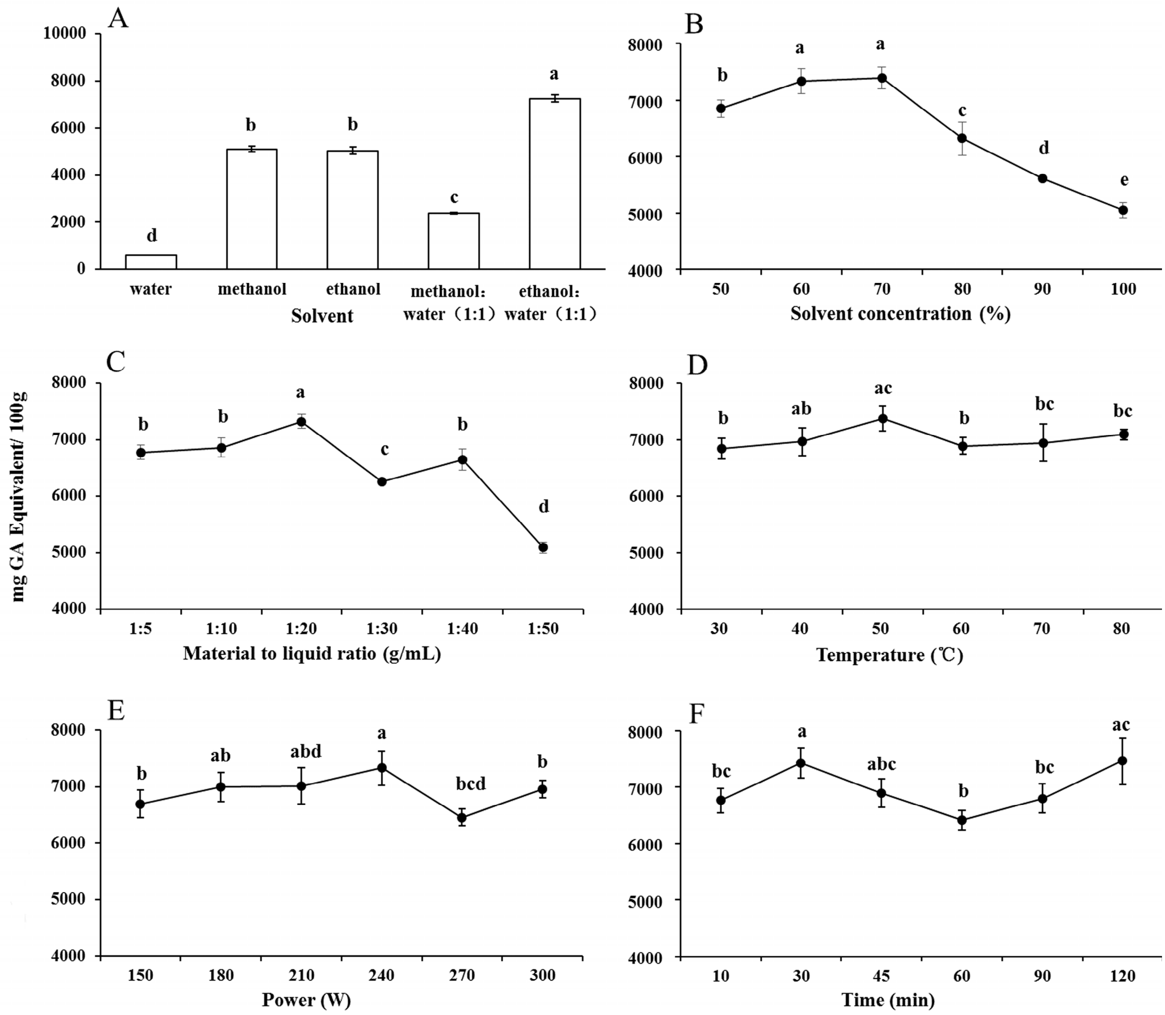

Figure 1. The effect of solvent type (A) and solvent concentration (B) extracted at 240 W, 50 °C and 30 min, with material to liquid ratio at 1:20 g/mL, material to liquid ratio (C, extracted at 240 W, 50 °C, 30 min, and 70% aqueous ethanol), extraction temperature (D, 240 W, 30 min, 70% aqueous ethanol, and 1:20 g/mL), sonication power (E, 50 °C, 30 min, 70% aqueous ethanol, and 1:20 g/mL), and extraction time (F, 240 W, 50 °C, 70% aqueous ethanol, and 1:20 g/mL) on the yields of total phenols in ATL by single factor test. Extraction was repeated thrice. Values marked by the same letter are not significantly different ($P < 0.05$).

2.1.2. Solvent concentration

Aqueous ethanol of different concentrations was used to conduct the single factor analysis under the following uniform conditions for material-to-liquid ratio, extraction temperature, ultrasonic power, and extraction time at 1:20 g/mL, 50 °C, 240 W, and 30 min, respectively. As shown in Figure 1B, phenolic yield increased from 6850.04 mg GAE/100 g d.w. to 7329.02 at ethanol concentration between 50% and 60%, and to the maximum (7388.07) at 70%. The efficiency then decreased with

Peer-reviewed version available at Molecules 2017, 22, 232; doi:10.3390/molecules22020232

further increase of ethanol concentrations, and reach the minimum (5026.35) at 100%. Therefore, it can be concluded that the aqueous ethanol exhibited the closest polarity to the phenols in ATL at the range between 60 and 80% as the efficiency reached the maximum value with ethanol concentration at 70%. Thus, the variable range of ethanol concentration used in the RSM experiments was 60-80%.

2.1.3. Material-to-liquid ratio

Phenolic yields with different material-to-liquid ratios were evaluated in the single factor analysis under the following uniform conditions for aqueous ethanol concentration, extraction temperature, ultrasonic power, and extraction time at 70%, 50 °C, 240 W, and 30 min, respectively. As shown in Figure 1C, phenolic yield increased slightly from 6772.95 mg GAE/100 g d.w. to 6858.25 at ratios between 1:5 and 1:10, and much rapidly to the maximum (7320.00) at 1:20. The efficiency declined at ratios between 1:20 and 1:30, then increased to a second peak at 1:40 and reached the minimum (5086.68) at 1:50. Based on the mass transfer principles occurred in UAE, the driving force for mass transfer is considered to be the concentration gradient between the solid and solvent [37]. These results revealed that the optimal ratio leading to the strongest driving force was 1:20 g/mL for phenolic extraction in ATL. Thus, the variable range of material-to-liquid ratio used in the RSM experiments was determined as 1:15 - 1:25 g/mL.

2.1.4. Extraction temperature

To study the effect of extraction temperature on phenolic yield, UAE was implemented at different temperatures under the following uniform conditions for ethanol concentration, material-to-liquid ratio, ultrasonic power, and extraction time at 70%, 1:20 g/mL, 240 W, and 30 min, respectively. As shown in Figure 1D, phenolic yield increased from the minimum (6840.00 mg GAE/100 g d.w.) at 30 °C to the maximum (7376.17) at 50 °C, decreased to 6890.21 at 60 °C, then slightly increased up to 80 °C thereafter with no significant differences between 60 and 80 °C. These results suggest that a relative high temperature increased phenolic extraction efficiency as it increased the number of cavitation nucleus formed [38], leading an enhanced mass transfer and therefore a better access of solvent to cell components [39]. However, this increase declined, namely, brought a negative effect on the efficiency when the temperature exceeded a certain value. This was mainly due to the decreased cavitation intensity under increased temperatures [40,41]. In addition, the accelerated evaporation would also be induced at high temperatures, which led to the decrease of driving force [42]. The yield affected by temperature with the same pattern in a UAE process were previously reported, such as phenols from olive fruit [11], oil from pomegranate seed [42], and carotene from citrus peels [43]. Thus, an extraction temperature range from 40 to 60 °C was chosen in RSM process of ATL.

2.1.5. Ultrasonic power

The effect of ultrasonic power on phenolic yield was determined under the following uniform conditions for ethanol concentration, material-to-liquid ratio, extraction temperature, and extraction time at 70%, 1:20 g/mL, 50 °C, and 30 min, respectively. As shown in Figure 1E, phenolic yield increased from 6693.94 mg GAE/100 g d.w. at 150 W to the maximum (7327.12) at 240 W. The yield decreased to the minimum (6456.36) at 270 W, then increased to 6959.13 at 300 W. There exhibited no significant differences among 150, 180, and 210 W or between 270 and 300 W. According to a report by Hemwimol et al. [44], with the larger amplitude ultrasonic wave traveling through extraction solvent, more bubbles would be created, and more collapse and violent shock wave and high-speed jet might be generated to disrupt the cell walls. Therefore, the penetration of extraction solvent into cells became stronger, resulting in more release of target components from cells into the mass medium. Consequently, the mass transfer rate was thus enhanced and led to an appropriate increase in yield. However, extraction efficiency tended to decrease when ultrasonic power was higher than 240 W, and this might be caused by degradation of bioactive compounds and overproduced bubbles which could hamper the propagation of ultrasound waves at a too high ultrasonic power [45]. Thus, an ultrasonic power range from 210 to 270 W was chosen in RSM process of ATL.

2.1.6. Extraction time

The effect of extraction time on phenolic yield was determined under the following uniform conditions for ethanol concentration, material-to-liquid ratio, extraction temperature, and ultrasonic power at 70%, 1:20 g/mL, 50 °C, and 240 W, respectively. As shown in Figure 1F, a biphasic increase in phenolic yield was observed with increases of the extraction time. Phenolic yield increased from 6760.65 mg GAE/100 g d.w. to 7421.41 with the sonication time prolonged from 10 to 30 min, then declined to the lowest (6411.25) at 60 min, and the yield increased again to the maximum (7458.61) at 120 min. There was no significant difference between phenolic yields at 10 and 30 min. The sonication time was recognized as a significant factor increasing the extraction efficiency on UAE process, however, extraction efficiency decreased in some cases due to a prolonged sonication time as it will lower the permeability of solvent into the cell walls due to oversuspended impurities [14]. Moreover, prolonged extraction time may increase the chances of decomposition of phenolics [46] and also potentially increase the loss of solvent by vaporization [47], which can directly affect the loss of mass transfer during extraction. Considering energy-saving, 30 min was chosen to conduct all the experimental design below.

2.2. Statistical analysis and model fitting

To optimize the operating parameters, all 30 random sequential experiments were performed under designed UAE conditions based on ranges of every single factors (independent variable) determined above to study the reciprocal influence of independent variables (i.e., solvent concentration, material-to-liquid ratio, extraction temperature and ultrasonic power) on the two dependent (response) variables (i.e., phenolic yield and its corresponding antioxidant activity). The experimental values, together with predicted values obtained by their response surface central composite design, were presented in Table 1.

Table 1. Response surface central composite design and experimental data and predicted values for extraction yield of phenols in ATL.

Run	Factors				Total phenols (mg/100 g)	DPPH (μmol/100 g)
	X_1 C (%)	X_2 R (g/L)	X_3 P (W)	X_4 T (ºC)	Experimental (Predicted) values	
1	70(0)	20(0)	240(0)	50(0)	7467.83 (7449.86)	71695.05 (72589.38)
2	60(-1)	15(-1)	270(1)	60(1)	7591.30 (7534.35)	70380.34 (70880.44)
3	70(0)	20(0)	240(0)	50(0)	7417.39 (7449.86)	73356.78 (72589.38)
4	80(1)	25(1)	270(1)	40(-1)	6622.83 (6632.18)	57161.41 (56161.13)
5	80(1)	25(1)	210(-1)	60(1)	6840.22 (6732.65)	51733.24 (52828.09)
6	80(1)	15(-1)	270(1)	60(1)	7005.87 (6927.40)	66300.47 (65584.34)
7	60(-1)	15(-1)	210(-1)	40(-1)	7281.30 (7204.18)	64060.73 (63443.39)
8	60(-1)	25(1)	270(1)	40(-1)	7180.98 (7062.72)	60133.24 (61057.29)
9	70(0)	20(0)	240(0)	70(2)	7384.35 (7425.71)	63223.73 (62238.86)
10	60(-1)	15(-1)	270(1)	40(-1)	7158.91 (7192.11)	60282.07 (59038.22)
11	60(-1)	25(1)	210(-1)	40(-1)	7168.48 (7172.58)	68041.95 (68609.08)
12	70(0)	20(0)	240(0)	30(-2)	7037.83 (7125.72)	56420.30 (57524.26)
13	70(0)	20(0)	240(0)	50(0)	7256.52 (7449.86)	70844.41 (72589.38)
14	50(-2)	20(0)	240(0)	50(0)	6776.52 (6846.72)	57567.32 (56833.36)
15	80(1)	15(-1)	210(-1)	40(-1)	6609.78 (6505.13)	58025.57 (56190.23)
16	80(1)	25(1)	210(-1)	40(-1)	6772.83 (6774.90)	60425.89 (59955.71)
17	90(2)	20(0)	240(0)	50(0)	5783.04 (5842.09)	42030.84 (42883.89)
18	70(0)	10(-2)	240(0)	50(0)	7026.96 (7141.37)	66619.14 (67862.93)

Preprints (www.preprints.org) | NOT PEER-REVIEWED | Posted: 9 January 2017 doi:10.20944/preprints201701.0036.v1

Peer-reviewed version available at Molecules 2017, 22, 232; doi:10.3390/molecules22020232

19	70(0)	20(0)	300(2)	50(0)	7106.09 (7147.63)	69835.50 (68702.84)
20	60(-1)	25(1)	270(1)	60(1)	7148.64 (7178.92)	62292.05 (63978.39)
21	80(1)	15(-1)	210(-1)	60(1)	6625.54 (6688.92)	58877.87 (57983.73)
22	70(0)	20(0)	180(-2)	50(0)	6931.30 (7019.01)	67402.26 (68654.02)
23	70(0)	20(0)	240(0)	50(0)	7519.13 (7449.86)	72961.25 (72589.38)
24	70(0)	20(0)	240(0)	50(0)	7587.83 (7449.86)	72829.01 (72589.38)
25	70(0)	20(0)	240(0)	50(0)	7450.43 (7449.86)	73849.78 (72589.38)
26	80(1)	25(1)	270(1)	60(1)	6851.09 (6873.33)	56634.84 (57282.08)
27	70(0)	30(2)	240(0)	50(0)	7040.87 (7055.71)	65851.05 (64726.36)
28	80(1)	15(-1)	270(1)	40(-1)	6513.91 (6460.19)	54193.49 (55542.27)
29	60(-1)	25(1)	210(-1)	60(1)	7006.52 (7005.36)	64600.48 (63281.61)
30	60(-1)	15(-1)	210(-1)	60(1)	7346.74 (7263.01)	66185.78 (67037.04)

Upon applying multiple regression analysis to the experimental data, the final quadratic equation obtained in terms of actual factors was given below.

When the phenolic extraction efficiencies (Y_1) were considered as the response:

$$Y_1 = -9574.12 + 322.61X_1 + 126.39X_2 + 43.31X_3 - 4.91X_4 + 1.51X_1X_2 - 0.03X_1X_3 + 0.31X_1X_4 - 0.16X_2X_3 - 1.13X_2X_4 + 0.24X_3X_4 - 2.76X_1^2 - 3.51X_2^2 - 0.10X_3^2 - 0.44X_4^2$$

When the antioxidant capacities (Y_2) were considered as the response:

$$Y_2 = -78025.43 + 1807.32X_1 + 1586.92X_2 + 15.99X_3 + 713.92X_4 - 1.75X_1X_2 + 0.78X_1X_3 - 1.12X_1X_4 - 1.31X_2X_3 - 11.16X_2X_4 + 1.72X_3X_4 - 14.22X_1^2 - 15.76X_2^2 - 0.27X_3^2 - 7.95X_4^2$$

Where, X_1, X_2, X_3, X_4, Y_1, Y_2 were aqueous ethanol concentration, material-to-liquid ratio, extraction temperature, ultrasonic power, response of phenolic yield, response of antioxidant activity, respectively.

The linear effect of solvent concentration (X_1) was found to be significant for both response variables while X_4 was only significant for phenol yield (Y_1), and X_2 and X_3 were only significant for antioxidant activity (Y_2). It can be concluded that solvent concentration was the vital parameter in both responses. However, the quadratic effect (X_1^2, X_2^2, X_3^2) was found to produce extremely significant ($P < 0.01$) positive effect on both Y_1 and Y_2, but X_4^2 was only significant for Y_2. ANOVA results for multiple regression analysis and response surface quadratic model of Y_1 and Y_2 were evaluated using the corresponding F and P values (Table 2). F values of Y_1 and Y_2 were calculated to be 25.95 and 50.34, both leading to a P value < 0.0001, suggesting that both the models were statistically extremely significant. The models' coefficient of determination (R^2) were 0.9604 and 0.9792, indicating that more than 96.04% and 97.92% of the response variability is explained, and supporting a good accuracy and ability of the established model within the range limits used [48]. Correlation coefficients of 0.9800 and 0.9898 also indicate a good positive correlation between the actual data and the predicted values obtained using CCD. The F-values of Lack of Fit of Y_1 and Y_2 were 0.6032 and 0.2015, respectively, implying that the Lack of Fit is not significantly relative to the pure error, thus the model can be used to predict the phenols and corresponding antioxidant activity of ATL. In addition, Adj-R^2, Pre-R^2 and the coefficient of variation (C.V.) were calculated to check the model's adequacy. Pre-R^2 of Y_1 and Y_2 were 0.8341 and 0.8968, which were in reasonable agreement with their Adj-R^2 of 0.9233 and 0.9597, respectively (Adj-R^2 – Pre-R^2 < 0.2), indicating a high degree of correlation between the measured and predicted data from the regression model [49]. The C.V. expressed the standard deviation as a percentage of the mean, and was found to be 1.5169% (< 5.00%) for the phenolic yield, and 2.3491% (< 5.00%) for antioxidant activity, implying that the models were reproducible [24]. Adequate precision measures the signal to noise ratio, which is desirable when the value is larger than 4. The ratios of 22.3775 and 28.1801 both referred an adequate signal and illustrated that the models (Y_1 and Y_2) were applicative for the present UAE process [50]. These correlation analyses between predicted values and actual data can be used to evaluate the suitability of the response surface model [51]. Thus, the model can be used to predict the phenolic yield and corresponding antioxidant activity under various extraction conditions during UAE process.

Preprints (www.preprints.org) | NOT PEER-REVIEWED | Posted: 9 January 2017 doi:10.20944/preprints201701.0036.v1

Peer-reviewed version available at Molecules 2017, 22, 232; doi:10.3390/molecules22020232

Table 2. Analysis of variance for the extraction of phenols yield (Y_1) and antioxidant capacity (Y_2).

	Source	Coefficient estimate	Sum of squares	Degree of freedom	Standard error	Mean square	F-value	P-value
Y_1	Model	7449.86	4.16E+06	14	43.66	2.97E+05	25.95	< 0.0001**
	X_1	-251.16	1.51E+06	1	21.83	1.51E+06	132.36	< 0.0001**
	X_2	-21.42	1.10E+04	1	21.83	1.10E+04	0.96	0.3422
	X_3	32.15	2.48E+04	1	21.83	2.48E+04	2.17	0.1614
	X_4	75	1.35E+05	1	21.83	1.35E+05	11.8	0.0037**
	X_1X_2	75.34	9.08E+04	1	26.74	9.08E+04	7.94	0.0130*
	X_1X_3	-8.22	1.08E+03	1	26.74	1.08E+03	0.09	0.7628
	X_1X_4	31.24	1.56E+04	1	26.74	1.56E+04	1.37	0.2609
	X_2X_3	-24.45	9.56E+03	1	26.74	9.56E+03	0.84	0.375
	X_2X_4	-56.51	5.11E+04	1	26.74	5.11E+04	4.47	0.0517
	X_3X_4	70.85	8.03E+04	1	26.74	8.03E+04	7.02	0.0182*
	X_1^2	-276.36	2.09E+06	1	20.42	2.09E+06	183.16	< 0.0001**
	X_2^2	-87.83	2.12E+05	1	20.42	2.12E+05	18.5	0.0006**
	X_3^2	-91.63	2.30E+05	1	20.42	2.30E+05	20.14	0.0004**
	X_4^2	-43.54	5.20E+04	1	20.42	5.20E+04	4.55	0.05
	Residual		1.72E+05	15		1.14E+04		
	Lack of Fit		1.09E+05	10		1.09E+04	0.87	0.6032
	Pure Error		6.26E+04	5		1.25E+04		
	Cor Total		4.33E+06	29				
	R^2	0.9604						
	Adj R^2	0.9233						
	Pred R^2	0.8341						
	Adeq Precision	22.3775						
	C.V. %	1.5169						
	r	0.98						
Y_2	Model	72589.38	1.57E+09	14	608.6	1.12E+08	50.34	< 0.0001**
	X_1	-3487.37	2.92E+08	1	304.3	2.92E+08	131.34	< 0.0001**
	X_2	-784.14	1.48E+07	1	304.3	1.48E+07	6.64	< 0.0001**
	X_3	12.2	3.57E+03	1	304.3	3.57E+03	0	0.0210*
	X_4	1178.65	3.33E+07	1	304.3	3.33E+07	15	0.9685
	X_1X_2	-350.05	1.96E+06	1	372.69	1.96E+06	0.88	0.0015**
	X_1X_3	939.3	1.41E+07	1	372.69	1.41E+07	6.35	0.3625
	X_1X_4	-450.04	3.24E+06	1	372.69	3.24E+06	1.46	0.0235*
	X_2X_3	-786.65	9.90E+06	1	372.69	9.90E+06	4.46	0.2459
	X_2X_4	-2230.28	7.96E+07	1	372.69	7.96E+07	35.81	0.052
	X_3X_4	2062.14	6.80E+07	1	372.69	6.80E+07	30.62	< 0.0001**
	X_1^2	-5682.69	8.86E+08	1	284.65	8.86E+08	398.56	< 0.0001**
	X_2^2	-1573.68	6.79E+07	1	284.65	6.79E+07	30.56	< 0.0001**
	X_3^2	-977.74	2.62E+07	1	284.65	2.62E+07	11.8	< 0.0001**
	X_4^2	-3176.95	2.77E+08	1	284.65	2.77E+08	124.57	0.0037**
	Residual		3.33E+07	15		2.22E+06		< 0.0001**
	Lack of Fit		2.71E+07	10		2.71E+06	2.18	0.2015
	Pure Error		6.22E+06	5		1.24E+06		0.2015
	Cor Total		1.60E+09	29				
	R^2	0.9792						
	Adj R^2	0.9597						
	Pred R^2	0.8968						
	Adeq Precision	28.1801						
	C.V. %	2.3491						
	r	0.9898						

* $0.01 \le P < 0.05$; ** $P < 0.01$

As shown in Table 1, the levels of phenolic yield ranges from 5783.04 to 7591.30 mg GAE/100 g d.w., and the levels of antioxidant activity ranges from 42030.84 to 73849.78 μmol TE/100 g d.w.. The

Preprints (www.preprints.org) | NOT PEER-REVIEWED | Posted: 9 January 2017 doi:10.20944/preprints201701.0036.v1

Peer-reviewed version available at *Molecules* **2017**, *22*, 232; doi:10.3390/molecules22020232

high levels of phenolic yield (7256.52 to 7587.83 mg GAE/100 g d.w.) and antioxidant activity (70844.41 to 73849.78 µmol TE /100 g d.w.) were obtained under the center point combinations of 70% ethanol, material-to-liquid ratio of 1:20 g/mL, 240 W, 50 °C, and 30 min. Moreover, the conditions, solvent concentration 66.21%, material-to-liquid ratio 1:15.31 g/mL, ultrasonic temperature 60 °C, power 267.30 W, and extraction time 30 min were predicted to provide the highest phenolic yield, together with the highest antioxidant activity according to the models fitted.

To further verify the models obtained from RSM, ATL was extracted under the predicted optimal UAE conditions, and its phenolic yield and antioxidant ability were evaluated and compared to the predicted maximum yield. For operational convenience, the optimal parameters were modified slightly in the verification experiment as follows: solvent concentration 66.20%, material-to-liquid ratio 1:15.30 g/mL, ultrasonic power 270.00 W, temperature 60 °C, and extraction time 30min. The predicted phenolic yield and antioxidant activity under the optimal conditions were 7589.19 mg GAE/100 g and 74010 µmol TE/ 100 g, and the experimental values under the optimal conditions were 7579.56 ± 354.44 mg GAE/100 g and 73585.78 ± 790.74 µmol TE/ 100 g, respectively. No significant differences were observed between predicted and experimental values ($P > 0.05$), indicating that the experimental results confirmed the adequate fitness of the predicted model.

2.3. Effect of interactions among variables on phenolic yield and antioxidant activity in ATL

To visualize interactions of two operational parameters on extraction efficiency, the responses were generated as triaxial response surfaces (Figure 2) and planar contour plots (Figure 3). Two variables unshown in the Figures were kept constant at their respective central experimental values and the other two variables presented on the two horizontal axis varied within their experimental ranges in order to understand their main and interactive effects on the dependent variables. Figs. 2a-f and 3a-f show the results of interactive influence of solvent concentration, material-to-liquid ratio, extraction temperature, and ultrasonic power on phenolic yield, while Figs. 2g-h and 3g-h exhibited the impact of these variables on antioxidant activity.

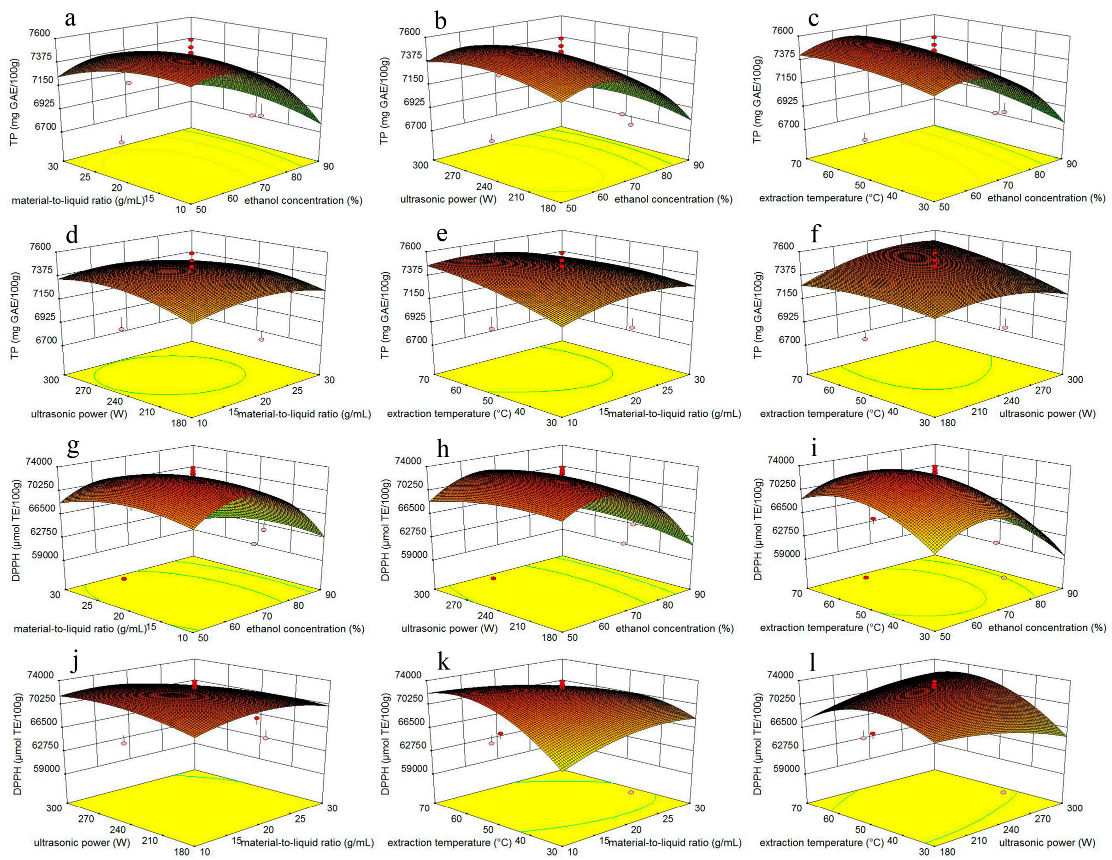

Preprints (www.preprints.org) | NOT PEER-REVIEWED | Posted: 9 January 2017 doi:10.20944/preprints201701.0036.v1

Peer-reviewed version available at *Molecules* **2017**, *22*, 232; doi:10.3390/molecules22020232

Figure 2. Response surfaces showing the effects of four variables (solvent concentration, material to liquid ratio, ultrasonic power, and extraction temperature) and their interactions on extraction yield of total phenols (TP, a-f) and their DPPH• scavenging capacity (g-l). The other two variables in each of the Figures were kept constant at their respective central experimental values.

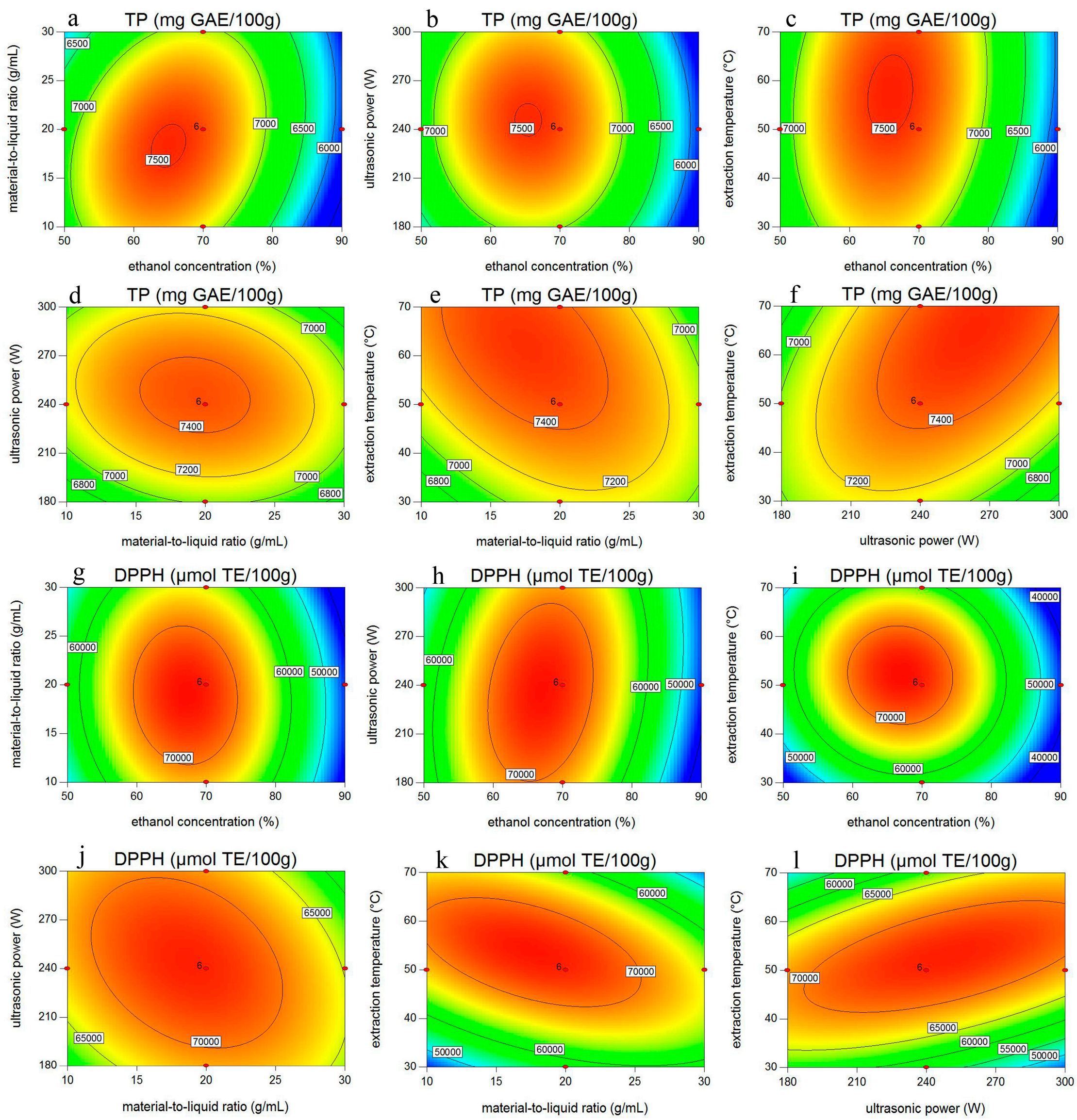

Figure 3. Contour plots showing the effects of four variables (solvent concentration, material to liquid ratio, ultrasonic power, and extraction temperature) and their interactions on extraction efficiency of total phenols (TP, a-f) and their DPPH• scavenging capacity (g-l). The other two variables in each of the Figures were kept constant at their respective central experimental values.

Figs. 2a-c, g-i and 3a-c, g-i show the phenols and antioxidant activities as responses of aqueous ethanol concentration (X_1) and the other factors (X_2, X_3, X_4). The extraction efficiencies first increased then decreased with increase of aqueous ethanol concentration from 50% to 90%, material-to-liquid ratio from 1:10 to 1:30 g/mL, ultrasonic power from 180 to 300 W, and extraction temperature from 30 to 70 °C.

The interaction of solvent concentration and material-to-liquid ratio (X_1X_2) showed extremely significant positive effect ($P < 0.001$) on both responses (see Table 2). At lower ethanol concentration with increasing material-to-liquid ratio, total phenols and antioxidant activity kept generally mild. However, the total phenols with antioxidant activity first increased, then decreased at lower material-

Peer-reviewed version available at Molecules 2017, 22, 232; doi:10.3390/molecules22020232

to-liquid ratio with increasing ethanol concentration (Figures 2a and g and 3a and g). The possible interaction mechanism between solvent concentration and material-to-liquid ratio might be interpreted as that the positive interaction caused by appropriate solvent concentration and material-to-liquid ratio affected the polarity and viscosity of aqueous ethanol and solubility of target phenolic compounds in the extraction solvent, thus influenced the yield of phenols.

As shown in Figures 2f and 2l, and 3f and 3l, the interaction between sonication power and temperature (X_3X_4) also showed significant positive effect ($P < 0.05$) on total phenols and antioxidant activity (Figures 2f and 3f). The possible interaction mechanism between temperature and power may be the change of cavitation threshold affected by changing temperature, which is responsible for acoustic cavitation and also results in the formation of a cavitational nucleus. The influence of relatively greater forces ruptures and erupts the formed cavitational nucleus and disrupts the cell tissues during extraction, which in turn enhances the mass transfer rate [39].

With respect to antioxidant activity (Y_2), the interaction effect of solvent concentration and sonication power (X_1X_4) was also found to be significant ($P < 0.05$). According to the study of Hemwimol et al. [44], only a small fraction of the electric energies from the ultrasound actually entered the extraction solvent in the ultrasonic bath system, and most of them were absorbed by the water in the bath. Under this circumstances, the rise of the solvent concentration might increase the utilization efficiency of the limited electric energies, then play a vital role in the improvement of the extraction yield.

2.4. Characterization of phenolic compositions in ATL

Table 3 shows a list of 29 phenolic compounds identified in ATL prepared under the optimal extraction conditions obtained above through UPLC–QTOF-MS/MS experiments, along with their retention times (RT), experimental m/z, calculated m/z, error values (ppm), molecular formula and MS/MS fragments. As signals in negative mode was stronger than those in the positive mode, data collected in negative mode was thus chosen to conduct the identification. Mass spectra in negative ion mode (Figure 4A), together with MS (Figure 4B) and MS/MS (Figure 4C) fragments of the peak with retention time at 26.51 min were presented as follows.

Peer-reviewed version available at Molecules 2017, 22, 232; doi:10.3390/molecules22020232

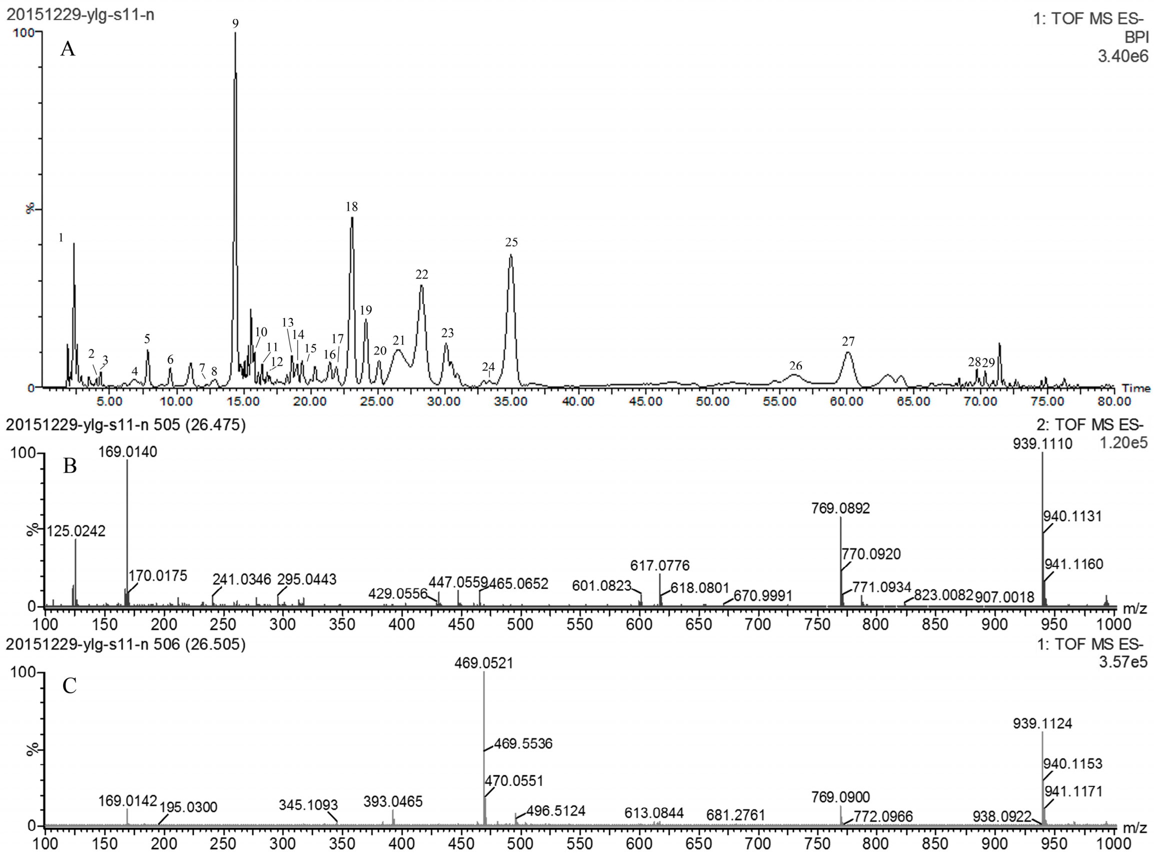

Figure 4. UPLC-QTOF-MS/MS data of the ATL extract obtained under the optimized conditions. Besides the UPLC-MS profile (A), a peak with the retention time at 26.51 min was identified as pentagalloyl glucose based on its MS (B) and MS/MS (C) fragments.

Table 3. Phenolic compounds tentatively identified in ATL by UPLC-QTOF-MS/MS analyses.

Peak	Rt (min)	[M-H]- (m/z)	Error (ppm)	Formula	MS/MS fragments m/z (% base peak)	Proposed compound
1	2.35	191.0564	4.2	$C_7H_{11}O_6$	127.0405(3.7), 111.0453(1.2)	Quinic acid
2	4.03	343.0654	-3.2	$C_{14}H_{15}O_{10}$	191.0559(28.0), 169.0139(100.0), 125.0243(73.3)	Theogallin
3	4.29	169.0143	3.5	$C_7H_5O_5$	125.0244(100), 169.0139(74.1)	Gallic acid
4	6.91	353.0864	-2.5	$C_{16}H_{17}O_9$	191.0552(100.0), 179.0348(53.0), 135.0449(69.3)	3-*O*-Caffeoylquinic acid
5	7.85	353.0862	-3.1	$C_{16}H_{17}O_9$	191.0550(100), 179.0339(54.7), 135.0444(68.0)	5-*O*-Caffeoylquinic acid
6	11.05	285.0612	0.7	$C_{12}H_{13}O_8$	153.0177(25.6), 109.0272(17.5)	Uralenneoside
7	12.64	337.0918	-1.5	$C_{16}H_{17}O_8$	191.0550(47.6), 163.0393(100.0), 119.0494(65.8)	*cis*-4-*p*-Coumaroylquinic acid
8	12.93	337.0923	0	$C_{16}H_{17}O_8$	191.0558(19.4), 163.0392(100.0), 119.0498(54.1)	*cis*-5-*p*-Coumaroylquinic acid
9	14.4	183.0323	16.4	$C_8H_7O_5$	183.0300(31.4), 124.0194(100.0)	4-*O*-Methyl-gallate
10	16.08	755.2031	-0.5	$C_{33}H_{39}O_{20}$	609.1443(54.7), 463.2144(11.2), 301.0345(21.1)	Quercetin-3-*O*-rhamninoside
11	16.39	289.0717	1.7	$C_{15}H_{13}O_6$	245.0822(32.9), 211.0291(7.7)	(+)-Catechin
12	16.91	863.1819	-0.5	$C_{45}H_{35}O_{18}$	289.0710(78.7)	cinnamtannin B1
13	18.65	479.0822	-0.8	$C_{21}H_{19}O_{13}$	316.0219(100.0), 287.0192(16.2), 271.0237(30.5)	Myricetin-*O*-hexoside I
14	19.01	479.0828	0.4	$C_{21}H_{19}O_{13}$	316.0221(100.0), 271.0249(28.5)	Myricetin-*O*-hexoside II
15	19.38	593.1513	1.2	$C_{27}H_{29}O_{15}$	593.1505(100.0), 447.0915(53.1), 301.0343(61.8)	Quercetin-3,7-*O*-α-L-dirhamnopyranoside
16	21.47	787.1001	0.9	$C_{34}H_{27}O_{22}$	615.0979(18.8), 465.0670(15.3), 169.0137(22.7)	1,2,3,6-Tetrakis-*O*-galloyl-β-D-glucose
17	21.95	449.0727	1.6	$C_{20}H_{17}O_{12}$	316.0228(100.0), 317.0274(24.4), 271.0247(37.8)	Myricetin-arabinoside/xylopyranoside Isomer
18	23.1	463.0878	0.2	$C_{21}H_{19}O_{12}$	316.0218(100.0), 287.0194(18.9)	Myricitrin
19	24.15	463.0877	0	$C_{21}H_{19}O_{12}$	300.0267(100.0), 255.0293(20.9)	Quercetin-3-*O*-galactoside
20	25.09	463.0884	1.5	$C_{21}H_{19}O_{12}$	300.0273(100.0), 255.0297(22.6)	Quercetin-3-*O*-glucoside (isoquercetin)
21	26.51	939.1124	2.1	$C_{41}H_{31}O_{26}$	769.0892(57.3), 617.0776(20.1), 447.0559(9.6), 169.0140(94.8)	Pentagalloyl glucose isomer
22	28.23	939.1109	0.5	$C_{41}H_{31}O_{26}$	769.0883(51.5), 617.0775(19.2), 447.0550(9.1), 169.0140(51.2)	Pentagalloyl glucose isomer
23	30.12	433.0768	-0.7	$C_{20}H_{17}O_{11}$	300.0271(100.0), 255.0286(26.8), 243.0291(10.4)	Quercetin-3-*O*-arabinopyranoside
24	33.32	433.0767	-0.9	$C_{20}H_{17}O_{11}$	300.0266(100.0), 271.0236(59.7), 255.0297(35.1)	Quercetin 3-*O*-arabinofuranoside
25	34.94	447.0927	0	$C_{21}H_{19}O_{11}$	300.0270(100.0), 271.0249(51.2), 255.0295(27.3)	Quercetin 3-*O*-rhamnoside
26	56.11	1091.12	-1	$C_{48}H_{35}O_{30}$	939.1072(60.0), 769.0875(22.8), 169.0133(100.0)	Hexagalloyl glucose
27	60.3	431.0974	-0.9	$C_{21}H_{19}O_{10}$	285.0387(100.0), 255.0288(59.4), 227.0336(34.9)	Kaempferol-3-*O*-α-L-rhamnoside
28	69.26	609.1234	-1.6	$C_{30}H_{25}O_{14}$	463.0871(68.8), 300.0274(95.3)	Quercetin-3-*O*-rutinoside
29	71.72	301.0354	2	$C_{15}H_9O_7$	301.0344(45.7), 243.0662(100.0)	Quercetin

Peer-reviewed version available at *Molecules* **2017**, 22, 232; doi:10.3390/molecules22020232

2.4.1. Gallates and gallotannins derivatives

Compound 2 (RT = 4.03 min) was identified as theogallin (a galloylquinic acid) with a $[M-H]^-$ ion at m/z 343.0654. It has a major fragment at m/z 191 (quinic acid) due to the loss of a galloyl moiety (152 amu) and another fragment at m/z 169 (gallic acid) due to the loss of a part of quinic acid moiety (174 amu). Compound 3 (4.29 min) gave a $[M-H]^-$ ion at 169.0143 and a major fragment ion at m/z 125 caused by the loss of a $-CO_2$ group, and was identified as gallic acid. Compound 4 was assigned as methyl gallate with a $[M-H]^-$ ion at m/z 183.0323 and a major fragment ion at m/z 124 due to the loss of $-CO_2CH_3$ (59 amu). The parent ions and MS/MS profiles of these three gallates accorded with the data reported in the literature [52].

Moreover, the gallic acid ion at m/z 169 occurred in not only compounds 2 and 3, but compounds 16, 21, 22, and 26, indicating that all these compounds share the gallic acid moiety. Compound 16 (21.47 min) with deprotonated ion at m/z 787.1001 was identified as tetra-*O*-galloyl-glucoside. It fragmented at m/z 615 with a loss of one gallic acid moiety (170), and fragmented at m/z 465 with another loss of a galloyl (152). Meanwhile, compounds 21 gave $[M-H]^-$ ion at m/z 939 with molecular formula $C_{41}H_{32}O_{26}$. It fragmented at m/z 769 with a loss of a gallic acid moiety (170), and fragmented at m/z 617 with another loss of galloyl (152) (Figure 4B and 4C). Thus compound 21 (26.51 min) was identified as a penta-*O*-galloyl-glucoside isomer. Possessing the same parent ion and fragments, compound 22 (28.23 min) was identified as another penta-*O*-galloyl-glucoside isomer. One of them should be the 1,2,3,4,6-pentakis-*O*-galloyl-β-D-glucose identified in ATL before [53]. Compound 26 (56.11 min) with deprotonated ion at m/z 1091.12 was identified as hexa-*O*-galloyl-glucoside. It fragmented at m/z 939 and 769 following the mode described above. The parent ions and fragmentation mode of these gallotannins were reported in the literature [54].

Accordingly, we hypothesized that there is a gallotannins pathway existing in the ATL, leading to the synthesis from gallic acid to tetra-*O*-galloyl-glucoside, penta-*O*-galloyl-glucoside and hexa-*O*-galloyl-glucoside. Grundhöfer et al. [55] elucidated the pathway forming complex gallotannins in *Rhus typhina* through enzyme studies. They reported the detailed converting process from gallic acid to β-glucogallin, digalloyglucose, trigalloyglucose, tetragalloyglucose, pentagalloylglucose, and hexagalloyglucose. As most of galloylglucoses mentioned above were also found in ATL, we conjectured the gallotannins pathway existing in ATL might be quite similar with the one in *Rhus typhina*. In addition, 1,2,3,4,6-pentakis-*O*-galloyl-β-D-glucose was the common precursor of two subclasses of hydrolyzable tannins, gallotannins and the related ellagitannins [52]. Thus the pathway from gallic acid to the penta-*O*-galloyl-glucoside might be the tip of the iceberg. Unfortunately, gallotannins with higher degree of polymerization than hexagalloyglucose was not found in the present study.

2.4.2. Flavonoids

Compound 29 (71.72 min) with a parent ion at m/z 301.0354 was identified as quercetin by comparing with the MS/MS data of a previous study [56]. Moreover, the quercetin moiety as a daughter ion at m/z 301 also existed in compounds 10, 15, 19, 20, 23, 24, 25, and 28, from which the abundance of quercetin derivatives in ATL could be inferred. Compound 10 (16.08 min) was assigned as quercetin 3-rhamninoside as its molecular ion was at m/z 755.2031 [57]. It fragmented at m/z 301 (quercetin) as its aglycone ion, and fragmented at m/z 609 due to the loss of a rhamnosyl (146 amu), and fragmented at m/z 463 due to another loss of a rhamnosyl. Compound 15 (19.38 min) was identified as quercetin-3,7-*O*-alpha-L-dirhamnopyranoside with a $[M-H]^-$ ion at 593.1513 and a daughter ion at 447 caused by the loss of a rhamnosyl (146 amu) [58]. According to Lin and Harnly [59], the glycosylated quercetin with a monosaccharide at the same position elute in C_{18} columns with the following order: galactoside, glucoside, xyloside, arabinopyranoside, arabinofuranoside, rhamnoside and glucuronide, and this order was further confirmed by Keinänen and Julkunen-Tiitto [60]. Thus compounds 19 (24.15 min), 20 (25.09 min), 23 (30.12 min), 24 (33.32 min), 25 (34.94 min), and 28 (69.26 min), with parent ions at m/z 463.0877, 463.0884, 433.0768, 433.0767, 447.0927, and 609.1234, respectively, were deduced as quercetin-3-*O*-galactoside (hyperoside), quercetin-3-*O*-glucoside (isoquercetin), quercetin-3-*O*-arabinopyranoside, quercetin-3-*O*-arabinofuranoside

Preprints (www.preprints.org) | NOT PEER-REVIEWED | Posted: 9 January 2017 doi:10.20944/preprints201701.0036.v1

Peer-reviewed version available at Molecules 2017, 22, 232; doi:10.3390/molecules22020232

(avicularin), quercetin-3-*O*-rhamnoside (quercitrin), and quercetin-3-*O*-rutinoside (rutin), respectively. Furthermore, by comparing their parent ions and fragments with those of literatures, the above deductions on compounds 19 [56], 20 [56], 25 [52], and 28 [58] were verified.

Compounds 13 and 14 shared a parent ion at m/z 479, and their common daughter ion at m/z 316 was assigned as myricetin moiety. According to Heras et al. [28], compounds 13 (18.65 min) and 14 (19.01 min) were identified as myricetin-*O*-hexoside I and myricetin-*O*-hexoside II, respectively. Besides compounds 13 and 14, compounds 17 and 18 also shared the myricetin moiety ion at m/z 316, thus they were considered as the myricetin derivatives. Compound 17 (21.95 min) with molecular ion at m/z 449.0727 was identified as myricetin-arabinoside/xylopyranoside as its MS/MS profile was corresponded with that of the literatures [27]. Compound 18 (23.10 min) was assigned as myricetrin-3-*O*-rhamnoside (myricitrin) with a $[M-H]^-$ ion at m/z 463.0878 and a aglycone ion at m/z 316 [61].

Compound 11 (16.39 min) was identified as catechin, as its molecular ion was at m/z 289.0717. It fragmented at m/z 245 and 211, corresponding with its MS/MS data in the literature [26]. Compound 27 (60.30 min) possessed a deprotonated ion at m/z 431.0974, and was identified as kaempferol-3-*O*-rhamnoside [58]. Its fragment ion at 285 was assigned as the kaempherol moiety.

2.4.3. Chlorogenic acid derivatives

Compound 1 (2.35 min) with deprotonated ion at m/z 191.0564 was identified as quinic acid by comparing its MS/MS data with the literature [29]. Quinic acid is a cyclic polyol, instead of phenol itself, however, it is an important part consisting caffeoylquinic acid derivatives. Compounds 4 (6.91 min) and 5 (7.85 min) were found to share a deprotonated ion at m/z 353, indicating the presence of monocaffeoylquinic acid isomers. According to Ncube et al. [62] and Melguizo-Melguizo et al. [29], the common base peak in their MS/MS spectra at m/z 191 illustrated the presence of quinic acid moiety, and the fragment ion at m/z 179 occurred in compound 4 indicated that caffeoyl group is linked to the 3-OH position of quinic acid. Therefore, compound 4 was identified as 3-*O*-caffeoylquinic acid while compound 5 was identified as 5-*O*-caffeoylquinic acid due to their different fragmentation pattern.

Compounds 7 (12.64 min) and 8 (12.93 min) were identified as *p*-coumaroylquinic acid isomers as they shared a deprotonated ion at m/z 337. According to Ncube et al. [62], *trans*- and *cis*-5-*p*-coumaroylquinic acids possess a base peak at m/z 191, while *trans*- and *cis*-4-*p*-coumaroylquinic acid own one at m/z 173. As they shared a base peak at m/z 191 in the present study, and considering their reported eluting order, compounds 7 and 8 were identified as *trans*- and *cis*-5-*p*-coumaroylquinic acids, respectively.

2.4.4. Other phenolic compounds

Compound 6 (11.05 min) with a molecular ion at m/z 285.0612 was identified as uralenneoside as it fragmented at m/z 153 due to the loss of hydroxybenzoic acid unit and at m/z 109 because of another loss of a CO_2 group from the carboxylic acid moiety, and its MS/MS data were accordance with the fragmentation pattern reported by Yu et al. [63]. Compound 12 (16.91 min), with deprotonated ion at m/z 863.1819, was identified as cinnamtannin B1 as it consisted of three epicatechin units, which was reflected by the daughter ion at m/z 289 [64].

To sum up, 29 phenolics identified were consisted of 7 gallates and gallotannins derivatives, 15 flavonoids (most flavonol-3-*O*-glycosides), 5 chlorogenic acid derivatives, and 2 other phenolic compounds. Previously, seven phenolic compounds were identified in ATL as gallic acid, quercetin, quercetin-3-arabinopyranoside [65], cholorogenic acid [3], methyl gallate [4], quercetin-3-*O*-L-rhamnoside [3], and 1,2,3,4,6-penta-*O*-galloyl-β-D-glucose [53]. To the best of our knowledge, the other 22 phenolics were firstly discovered in the present study. These findings not only signified the superiority of the UAE condition optimized, but also provided the fundamental information to characterization of the phenolic compositions in ATL.

3. Materials and Methods

3.1. Chemicals and plant materials

Folin-Ciocalteu reagents, 2,2-diphenyl-1-picrylhydrazyl (DPPH), and 6-hydroxy-2,5,7,8-tetramethylchroman-2-carboxylic acid (Trolox) were purchased from Sigma Chemical (USA). HPLC grade acetonitrile and formic acid were purchased from Fisher Scientific (USA). Ultra-pure water was prepared using a Milli-Q50 SP Reagent Water System (Millipore Corporation, USA). Other reagents (analytical grade) were purchased from Sinopharm Chemical Reagent Co. Ltd. (China).

Twenty *Acer truncatum* Bunge trees, whose tree-age (around 15 years old) and growth environment were approximatively identical, were randomly selected in Bajiajiaoye Park, Haidian District (N 40°00'57.21''; E 116°19'43.36'' with altitude 39-41 m) and authenticated by associate professor Zhonghua Liu, Beijing Forestry University, Beijing, China. *A. truncatum* leaves (ATL) were uniformly collected from the selected trees in April 20, 2015 and taken back to laboratory immediately. The leaves were cleaned with distilled water and air-dried, the dried leaves were grinded and passed a 250 × 250-μm sieve, and the powder was stored at -20 °C in refrigerator for extraction.

3.2. Optimization of UAE

3.2.1. Preliminary experiments

To test the impact of solvent type on phenolic yield, 1.000 g leaf powder was mixed thoroughly with different solvents, including water, methanol, ethanol, methanol: water (1:1, v:v) or ethanol: water (1:1, v:v) at a material-to-liquid ratio (g/mL) of 1:20 in a plastic centrifuge tube. The tube was then immersed into a tunable ultrasonic cleaning bath (KQ-300DE type, Kunshan Ultrasonic Instrument Co., Ltd., China) with the liquid level in the tube keeping lower than that of the cleaner tank, and extracted under ultrasonic conditions at 50 °C, 240 W and 30 min. The sample mixture was then centrifuged for 10 min at 6000 rpm and the supernatant was collected. The resulting residue were repeated for extraction twice more, and all the supernatants were combined, filtered, and diluted to a final volume of 60 mL. The resulting solutions were analyzed for total phenols. The optimal solvent with the highest total phenol content was selected for the following experiments.

Effect of each independent variable on phenolic yield was determined by single factor experimental designs. ATL was extracted with the optimal solvent selected and different concentrations (50, 60, 70, 80, 90 and 100%), material-to-liquid ratios (1:5, 1:10, 1: 20, 1:30, 1:40, 1:50 g/mL), ultrasonic powers (150, 180, 210, 240, 280 and 300 W), sonication temperatures (30, 40, 50, 60, 70 and 80 °C) and sonication time (10, 30, 45, 60, 90 and 120 min). Total phenols were determined as the parameter for assessment, and the levels of individual independent variables for CCD were obtained according to these single factor experiments.

3.2.2. RSM experiment

After the single factor tests, RSM with CCD was applied to estimate the effect of independent variables (i.e., X_1, extraction temperature; X_2, ultrasonic power; X_3, solvent concentration; X_4, liquid-to-material ratio) and their interactions on UAE of phenolic yield (Y_1) and antioxidant activity (Y_2). Based on preliminary single factor analysis and literature data, levels of independent parameters were selected and coded at five levels according to Eq. (1):

$$x_i = \frac{X_i - X_0}{\Delta X_i} \quad i = 1,2,3,4, \tag{1}$$

Where x_i and X_i are the coded and actual values of an independent variable, respectively. X_0 is the actual value on the center point of X_i, and ΔX_i is the value of the step change. The design values of independent variables and their coded values are represented in Table 4. In the present study, CDD conducted 30 experimental points including six replicates at the central point, sixteen factorial points and eight axial points for a full factorial design to study the effect of independent variables on the response. The experiments were randomized and the response values in each trial were analyzed using Design-Expert (Version 8.0.6, Stat-Ease Inc., Minneapolis, USA) and fitted to a second-order

Preprints (www.preprints.org) | NOT PEER-REVIEWED | Posted: 9 January 2017 doi:10.20944/preprints201701.0036.v1

Peer-reviewed version available at Molecules 2017, 22, 232; doi:10.3390/molecules22020232

polynomial regression model expressing mathematical relationship between independent variables (X_1, X_2, X_3 and X_4) and responses (Y_1 and Y_2):

$$Y = \beta_0 + \sum_{i=1}^{4} \beta_i X_i + \sum_{i=1}^{3} \sum_{j=i+1}^{4} \beta_{ij} X_i X_j + \sum_{i=1}^{4} \beta_{ii} X_i^2, \quad (2)$$

where, Y (Y_1 or Y_2) is the predicted response, X_i and X_j are diverse input variables that influence the response variable Y, β_0 is the constant coefficient, β_i is the linear coefficient, β_{ij} is the interaction coefficient of two factors (X_i and X_j), and β_{ii} is the quadratic coefficient of one factor (X_i^2).

Table 4. Independent variables and their levels and corresponding coded values used in CCD.

Independent variables	**Independent levels**				
	-2	**-1**	**0**	**1**	**2**
Solvent concentration, X_1 (%)	50	60	70	80	90
Material-to-liquid ratio, X_2 (g/mL)	1:5	1:15	1:20	1:25	1:30
Extraction temperature, X_3 (ºC)	30	40	50	60	70
Sonication power, X_4 (W)	180	210	240	270	300

The obtained model was verified by comparing the phenolic yield and antioxidant ability of the ATL extract obtained under the optimal UAE conditions to those predicted by the models. Furthermore, the resulting solution was analysis by UPLC-QTOF-MS/MS for its phenolic compositions.

3.3. Measurement of total phenols

Total phenols were determined according to the Folin–Ciocalteu method [31] with slight modifications. In brief, 40 μL of 25% Folin–Ciocalteu solution was added to designated wells of a 96-well microplate, followed by addition of 20 μL standard (10-400 mg/L gallic acid, R^2 = 0.999), ATL extract solution or blank (MilliQ water). After blending, 140 μL of 700 mM Na_2CO_3 solution was added to each well, and the plate was shaken for 5 min at 250 rpm and incubated in dark at 40 °C for 30 min, followed by absorbance measurement at 765 nm with a microplate reader (Bio-Rad xMark™ Microplate Absorbance Spectrophotometer, USA). Results were expressed as mg gallic acid equivalent (GAE)/100 g d.w. of ATL powder.

3.4. Determination of DPPH• scavenging activity

Assays of DPPH• scavenging activity were performed using the method described by Alañón et al. [32] with slight modifications. In brief, 10 μL standard (0-400 mg/L, R^2 = 0.998), ATL extract solution or blank was added to a designated well of a 96-well microplate. Subsequently, 40 μL of 1 mM freshly prepared DPPH solution was added to each well followed by addition of 190 μL methanol, and the plate was then stood in an orbital shaker setting at 200 rpm for 1 min. After 30 min incubation at room temperature in dark, absorbance was recorded at 517 nm using the microplate reader. Results were expressed as μmol Trolox equivalent (TE)/100 g d.w. of ATL powder.

3.5. UPLC-QTOF-MS/MS analyses of phenolic compositions

The UPLC-QTOF-MS/MS system was comprised of an Acquity Ultra-performance Liquid Chromatography (UPLC) system (Waters, USA) and a QTOF-MS mass spectrometer (Xevo G2-XS, Waters, USA). A C_{18} column (Diamonsil C_{18} 5μm 250 × 4.6 mm i.d., Dikma, China) was used for separation, and the column temperature was set at 30 °C. The mobile phase was consisted of water with 0.4% formic acid (v:v) (A) and acetonitrile (B) under the following gradient program: 0-10 min, 10% B; 10-12 min, 10-18% B; 12-33 min, 18% B; 33-35 min, 18-15% B; 35-40 min, 15% B; 40-42 min, 15-18% B; 42-60 min, 18% B; 60-80 min, 18-50% B. The flow rate was set at 1 mL/min with an injection volume of 10 μL. Mass spectra were recorded in the range of m/z 100–1500. MS experiments were performed both in positive and negative ionization mode under the following conditions: nitrogen drying gas flow, 10.0 L/min; nebulizer pressure, 45 psi; gas drying temperature, 370 °C; capillary and fragmentor voltage, 2.500 KV; and with MS/MS collision energies set at 20 V. Peak identification was performed by comparing the mass spectra and fragmentation ions with data from reported literatures.

3.6. Statistical analysis

Experiment design was performed using Design-Expert (Version 8.0.6, Stat-Ease Inc., Minneapolis, USA). All experimental results obtained were expressed as means ± SD, and data were analyzed by analysis of variance ($P < 0.05$) using SPSS software (Version 22.0, SPSS Inc., Chicago, IL, USA). All analyses were performed in triplicate.

4. Conclusions

The current study is the first report on the ultrasonic stimulation for phenolic yield and antioxidant activity in ATL. The quadratic model well fitted both responses, i.e., total phenol yield and antioxidant activity. Operating parameters were optimized using single factor experiments and response surface design. Optimal conditions were found to be percentage of aqueous ethanol 66.21%, material-to-liquid ratio 1:15.25 g/mL, extraction temperature 60 °C; ultrasonic power 270 W, and ultrasound time 30 min, which gave a maximum total phenol yield of 7593.62 mg GAE equivalent /100 g d.w. and antioxidant activity of 74241.61 μmol TE/100 g d.w.. And the verified results confirmed the adequate fitness of the predicted model. Furthermore, 22 phenolic compounds were first discovered in the present study with UPLC-QTOF-MS/MS analysis, which indicated the superiority of the extraction condition and provided new insights to the phenolic compositions of ATL.

Acknowledgments: This work was financially supported by the Fundamental Research Funds for the Central Universities (No. BLYJ201412), and the Ph.D. Programs Foundation of Ministry of Education (20120014110006), China. The funders played no role in the study design, data collection or analysis, our decision to publish, or preparation of the manuscript.

Author Contributions: Lingguang Yang, Peipei Yin, Liwei Sun and Yujun Liu conceived and designed the experiments, performed the experiments, analyzed the data and wrote the paper. Hang Fan, Qiang Xue, Ke Li and Xiang Li participated in the experiments. Yujun Liu provided facilities and reviewed the manuscript. All authors read and approved the final manuscript.

Conflicts of Interest: The authors declare no conflict of interest.

References

1. Guo, X.; Wang, R.; Chang, R.; Liang, X.; Wang, C.; Luo, Y.; Yuan, Y.; Guo, W., Effects of nitrogen addition on growth and photosynthetic characteristics of Acer truncatum seedlings. *Dendrobiology* **2014**, 72, 151-161.
2. More, D.; White, J., Cassell's trees of Britain and Northern Europe. Cassells Trees of Britain & Northern Europe **2003**.
3. Ma, X.; Tian, W.; Wu, L.; Cao, X.; Ito, Y., Isolation of quercetin-3-O-l-rhamnoside from Acer truncatum Bunge by high-speed counter-current chromatography. *J. Chromatogr. A* **2005**, 1070, (1-2), 211-214.
4. Ma, X.; Wu, L.; Ito, Y.; Tian, W., Application of preparative high-speed counter-current chromatography for separation of methyl gallate from Acer truncatum Bunge. *J. Chromatogr. A* **2005**, 1076, (1-2), 212-215.
5. Wu, D.; Wu, X. D.; You, X. F.; Ma, X. F.; Tian, W. X., Inhibitory effects on bacterial growth and beta-ketoacyl-ACP reductase by different species of maple leaf extracts and tannic acid. *Phytother. Res.* **2010**, 24 Suppl 1, S35-41.
6. Zhang, F.; Luo, S. Y.; Ye, Y. B.; Zhao, W. H.; Sun, X. G.; Wang, Z. Q.; Li, R.; Sun, Y. H.; Tian, W. X.; Zhang, Y. X., The antibacterial efficacy of an aceraceous plant [Shantung maple (Acer truncatum Bunge)] may be related to inhibition of bacterial beta-oxoacyl-acyl carrier protein reductase (FabG). *Biotechnol. Appl. Bioc.* **2008**, 51, (Pt 2), 73-8.
7. Zhao, W. H.; Gao, C.; Zhang, Y. X.; Tian, W. X., Evaluation of the inhibitory activities of aceraceous plants on fatty acid synthase. *J. Enzym. Inhib. Med. Ch.* 2007, 22, (4), 501-10.

8. Zhao, W. H.; Zhang, J. F.; Zhe, W.; Zhang, Y. X.; Tian, W. X., The extract of leaves of Acer truncatum Bunge: A natural inhibitor of fatty acid synthase with antitumor activity. *J. Enzym. Inhib. Med. Ch.* **2006**, 21, (5), 589-96.
9. Chemat, F.; Zill e, H.; Khan, M. K., Applications of ultrasound in food technology: Processing, preservation and extraction. *Ultrason. Sonochem.* **2011**, 18, (4), 813-35.
10. Yuan, J.; Huang, J.; Wu, G.; Tong, J.; Xie, G.; Duan, J.-a.; Qin, M., Multiple responses optimization of ultrasonic-assisted extraction by response surface methodology (RSM) for rapid analysis of bioactive compounds in the flower head of Chrysanthemum morifolium Ramat. *Ind. Crop. Prod.* **2015**, 74, 192-199.
11. Jerman, T.; Trebše, P.; Mozetič Vodopivec, B., Ultrasound-assisted solid liquid extraction (USLE) of olive fruit (Olea europaea) phenolic compounds. *Food Chem.* **2010**, 123, (1), 175-182.
12. Tchabo, W.; Ma, Y.; Engmann, F. N.; Zhang, H., Ultrasound-assisted enzymatic extraction (UAEE) of phytochemical compounds from mulberry (Morus nigra) must and optimization study using response surface methodology. *Ind. Crop. Prod.* **2015**, 63, 214-225.
13. Xu, J.; Wang, W.; Liang, H.; Zhang, Q.; Li, Q., Optimization of ionic liquid based ultrasonic assisted extraction of antioxidant compounds from Curcuma longa L. using response surface methodology. *Ind. Crop. Prod.* **2015**, 76, 487-493.
14. Xu, G.; Liang, C.; Huang, P.; Liu, Q.; Xu, Y.; Ding, C.; Li, T., Optimization of rice lipid production from ultrasound-assisted extraction by response surface methodology. *J. Cereal Sci.* **2016**, 70, 23-28.
15. Wu, H.; Zhu, J.; Diao, W.; Wang, C., Ultrasound-assisted enzymatic extraction and antioxidant activity of polysaccharides from pumpkin (Cucurbita moschata). *Carbohyd. Polym.* **2014**, 113, 314-24.
16. Zhang, H.; Ma, H.; Liu, W.; Pei, J.; Wang, Z.; Zhou, H.; Yan, J., Ultrasound enhanced production and antioxidant activity of polysaccharides from mycelial fermentation of Phellinus igniarius. *Carbohyd. Polym.* **2014**, 113, 380-7.
17. Valdez-Flores, M.; Germán-Báez, L. J.; Gutiérrez-Dorado, R.; Medina-Godoy, S.; Norzagaray-Valenzuela, C.; Hernández-Verdugo, S.; Reyes-Moreno, C.; Valdez-Ortiz, A., Improving bioactivities of Jatropha curcas protein hydrolysates by optimizing with response surface methodology the extrusion cooking process. *Ind. Crop. Prod.* **2016**, 85, 353-360.
18. Ma, C. H.; Liu, T. T.; Yang, L.; Zu, Y. G.; Wang, S. Y.; Zhang, R. R., Study on ionic liquid-based ultrasonic-assisted extraction of biphenyl cyclooctene lignans from the fruit of Schisandra chinensis Baill. *Anal. Chim. Acta* **2011**, 689, (1), 110-6.
19. Hatambeygi, N.; Abedi, G.; Talebi, M., Method development and validation for optimised separation of salicylic, acetyl salicylic and ascorbic acid in pharmaceutical formulations by hydrophilic interaction chromatography and response surface methodology. *J. Chromatogr. A* **2011**, 1218, (35), 5995-6003.
20. Talebpour, Z.; Ghassempour, A.; Abbaci, M.; Aboul-Enein, H. Y., Optimization of Microwave-Assisted Extraction for the Determination of Glycyrrhizin in Menthazin Herbal Drug by Experimental Design Methodology. *Chromatographia* **2009**, 70, (1-2), 191-197.
21. Wang, T.; Liang, H.; Yuan, Q., Optimization of ultrasonic-stimulated solvent extraction of sinigrin from Indian mustard seed (Brassica Juncea L.) using response surface methodology. *Phytochem. Analysis* **2011**, 22, (3), 205-13.
22. Dayana Priyadharshini, S.; Bakthavatsalam, A. K., Optimization of phenol degradation by the microalga Chlorella pyrenoidosa using Plackett-Burman Design and Response Surface Methodology. *Bioresource Technol.* **2016**, 207, 150-6.
23. Elboughdiri, N.; Mahjoubi, A.; Shawabkeh, A.; Khasawneh, H. E.; Jamoussi, B., Optimization of the Degradation of Hydroquinone, Resorcinol and Catechol Using Response Surface Methodology. *Adv. Chem. Eng. Sci.* **2015**, 5, (2012), 111-120.
24. Samavati, V., Polysaccharide extraction from Abelmoschus esculentus: optimization by response surface methodology. *Carbohyd. Polym.* **2013**, 95, (1), 588-97.
25. Ahmadi, M.; Vahabzadeh, F.; Bonakdarpour, B.; Mehranian, M., Empirical modeling of olive oil mill wastewater treatment using loofa-immobilized Phanerochaete chrysosporium. *Process Biochem.* **2006**, 41, (5), 1148-1154.
26. Barnaba, C.; Dellacassa, E.; Nicolini, G.; Nardin, T.; Malacarne, M.; Larcher, R., Identification and quantification of 56 targeted phenols in wines, spirits, and vinegars by online solid-phase extraction - ultrahigh-performance liquid chromatography - quadrupole-orbitrap mass spectrometry. *J. Chromatogr. A* **2015**, 1423, 124-35.

Peer-reviewed version available at *Molecules* **2017**, *22*, 232; doi:10.3390/molecules22020232

27. Díaz-de-Cerio, E.; Gómez-Caravaca, A. M.; Verardo, V.; Fernández-Gutiérrez, A.; Segura-Carretero, A., Determination of guava (Psidium guajava L.) leaf phenolic compounds using HPLC-DAD-QTOF-MS. *J. Funct. Foods* **2016**, 22, 376-388.
28. Heras, R. M.-L.; Quifer-Rada, P.; Andrés, A.; Lamuela-Raventós, R., Polyphenolic profile of persimmon leaves by high resolution mass spectrometry (LC-ESI-LTQ-Orbitrap-MS). *J. Funct. Foods* **2016**, 23, 370-377.
29. Melguizo-Melguizo, D.; Diaz-de-Cerio, E.; Quirantes-Piné, R.; Švarc-Gajić, J.; Segura-Carretero, A., The potential of Artemisia vulgaris leaves as a source of antioxidant phenolic compounds. *J. Funct. Foods* **2014**, 10, 192-200.
30. Kolniak-Ostek, J., Identification and quantification of polyphenolic compounds in ten pear cultivars by UPLC-PDA-Q/TOF-MS. *J. Food Compos. Anal.* **2016**, 49, 65-77.
31. Sumczynski, D.; Bubelova, Z.; Sneyd, J.; Erb-Weber, S.; Mlcek, J., Total phenolics, flavonoids, antioxidant activity, crude fibre and digestibility in non-traditional wheat flakes and muesli. *Food Chem.* **2015**, 174, 319–325.
32. Alañón, M. E.; Castro-Vázquez, L.; Díaz-Maroto, M. C.; Gordon, M. H.; Pérez-Coello, M. S., A study of the antioxidant capacity of oak wood used in wine ageing and the correlation with polyphenol composition. *Food Chem.* **2011**, 128, (4), 997–1002.
33. Fu, Z.-f.; Tu, Z.-c.; Zhang, L.; Wang, H.; Wen, Q.-h.; Huang, T., Antioxidant activities and polyphenols of sweet potato (Ipomoea batatas L.) leaves extracted with solvents of various polarities. *Food Bioscience* **2016**, 15, 11-18.
34. Metrouh-Amir, H.; Duarte, C. M. M.; Maiza, F., Solvent effect on total phenolic contents, antioxidant, and antibacterial activities of Matricaria pubescens. *Ind. Crop. Prod.* **2015**, 67, 249-256.
35. Wijekoon, M. M. J. O.; Bhat, R.; Karim, A. A., Effect of extraction solvents on the phenolic compounds and antioxidant activities of bunga kantan (Etlingera elatior Jack.) inflorescence. *J. Food Compos. Anal.* **2011**, 24, (4-5), 615-619.
36. Cujic, N.; Savikin, K.; Jankovic, T.; Pljevljakusic, D.; Zdunic, G.; Ibric, S., Optimization of polyphenols extraction from dried chokeberry using maceration as traditional technique. *Food Chem.* **2016**, 194, 135-42.
37. Belwal, T.; Dhyani, P.; Bhatt, I. D.; Rawal, R. S.; Pande, V., Optimization extraction conditions for improving phenolic content and antioxidant activity in Berberis asiatica fruits using response surface methodology (RSM). *Food Chem.* **2016**, 207, 115-24.
38. Filgueiras, A. V.; Capelo, J. L.; Lavilla, I.; Bendicho, C., Comparison of ultrasound-assisted extraction and microwave-assisted digestion for determination of magnesium, manganese and zinc in plant samples by flame atomic absorption spectrometry. *Talanta* **2000**, 53, (2), 433-441.
39. Toma, M.; Vinatoru, M.; Paniwnyk, L.; Mason, T. J., Investigation of the effects of ultrasound on vegetal tissues during solvent extraction. *Ultrason. Sonochem.* **2001**, 8, (2), 137-142.
40. Entezari, M. H.; Kruus, P., Effect of frequency on sonochemical reactions II. Temperature and intensity effects. *Ultrason. Sonochem.* **1996**, 3, (1), 19-24.
41. Raso, J.; Mañas, P.; Pagán, R.; Sala, F. J., Influence of different factors on the output power transferred into medium by ultrasound. *Ultrason. Sonochem.* **1999**, 5, (4), 157-162.
42. Tian, Y.; Xu, Z.; Zheng, B.; Martin Lo, Y., Optimization of ultrasonic-assisted extraction of pomegranate (Punica granatum L.) seed oil. *Ultrason. Sonochem.* **2013**, 20, (1), 202-8.
43. Sun, Y.; Liu, D.; Chen, J.; Ye, X.; Yu, D., Effects of different factors of ultrasound treatment on the extraction yield of the all-trans-beta-carotene from citrus peels. *Ultrason. Sonochem.* **2011**, 18, (1), 243-9.
44. Hemwimol, S.; Pavasant, P.; Shotipruk, A., Ultrasound-assisted extraction of anthraquinones from roots of Morinda citrifolia. *Ultrason. Sonochem.* **2006**, 13, (6), 543-8.
45. Lou, Z.; Wang, H.; Zhang, M.; Wang, Z., Improved extraction of oil from chickpea under ultrasound in a dynamic system. *J. Food. Eng.* **2010**, 98, (1), 13-18.
46. Naczk, M.; Shahidi, F., Extraction and analysis of phenolics in food. *J. Chromatogr. A* **2004**, 1054, (1-2), 95-111.
47. Tan, M. C.; Tan, C. P.; Ho, C. W., Effects of extraction solvent system, time and temperature on total phenolic content of henna (Lawsonia inermis) stems. *Int. Food Res. J.* **2013**, 20, (6), 3117-3123.
48. Li, Y.; Fabiano-Tixier, A. S.; Tomao, V.; Cravotto, G.; Chemat, F., Green ultrasound-assisted extraction of carotenoids based on the bio-refinery concept using sunflower oil as an alternative solvent. *Ultrason. Sonochem.* **2013**, 20, (1), 12-8.

49. Erbay, Z.; Icier, F., Optimization of hot air drying of olive leaves using response surface methodology. *J. Food Eng.* **2009**, 91, (4), 533-541.
50. Jin, X.; Ning, Y., Extraction optimization and bioactivity of polysaccharides from Aspergillus fumigatus AF1. *Carbohyd. Polym.* **2013**, 96, (2), 411-6.
51. Prakash Maran, J.; Mekala, V.; Manikandan, S., Modeling and optimization of ultrasound-assisted extraction of polysaccharide from Cucurbita moschata. *Carbohyd. Polym.* **2013**, 92, (2), 2018-26.
52. Dorta, E.; González, M.; Lobo, M. G.; Sánchez-Moreno, C.; de Ancos, B., Screening of phenolic compounds in by-product extracts from mangoes (Mangifera indica L.) by HPLC-ESI-QTOF-MS and multivariate analysis for use as a food ingredient. *Food Res. Int.* **2014**, 57, 51-60.
53. Kiss, A. K.; Naruszewicz, M., Polyphenolic compounds characterization and reactive nitrogen species scavenging capacity of Oenothera paradoxa defatted seed extracts. *Food Chem.* **2012**, 131, (2), 485-492.
54. Grundhöfer, P.; Niemetz, R.; Schilling, G.; Gross, G. G., Biosynthesis and subcellular distribution of hydrolyzable tannins. *Phytochemistry* **2001**, 57, (6), 915-927.
55. Mocan, A.; Schafberg, M.; Crișan, G.; Rohn, S., Determination of lignans and phenolic components of Schisandra chinensis (Turcz.) Baill. using HPLC-ESI-ToF-MS and HPLC-online TEAC: Contribution of individual components to overall antioxidant activity and comparison with traditional antioxidant assays. *J. Funct. Foods* **2016**, 24, 579-594.
56. Cuoco, G.; Mathe, C.; Vieillescazes, C., Liquid chromatographic analysis of flavonol compounds in green fruits of three Rhamnus species used in Stil de grain. *Microchem. J.* **2014**, 115, 130-137.
57. Aguirre-Hernandez, E.; Gonzalez-Trujano, M. E.; Martinez, A. L.; Moreno, J.; Kite, G.; Terrazas, T.; Soto-Hernandez, M., HPLC/MS analysis and anxiolytic-like effect of quercetin and kaempferol flavonoids from Tilia americana var. mexicana. *J. Ethnopharmacol.* **2010**, 127, (1), 91-7.
58. Zhang, J.-l.; Cui, M.; He, Y.; Yu, H.-l.; Guo, D.-a., Chemical fingerprint and metabolic fingerprint analysis of Danshen injection by HPLC–UV and HPLC–MS methods. *J. Pharmaceut. Biomed.* **2005**, 36, (5), 1029-1035.
59. Keinänen, M.; Julkunen-Tiitto, R., High-performance liquid chromatographic determination of flavonoids in Betula pendula and Betula pubescens leaves. *J. Chromatogr. A* **1998**, 793, (2), 370-377.
60. Zhang, X.; Huang, H.; Zhao, X.; Lv, Q.; Sun, C.; Li, X.; Chen, K., Effects of flavonoids-rich Chinese bayberry (Myrica rubra Sieb. et Zucc.) pulp extracts on glucose consumption in human HepG2 cells. *J. Funct. Foods* 2015, 14, 144-153.
61. Ncube, E. N.; Mhlongo, M. I.; Piater, L. A.; Steenkamp, P. A.; Dubery, I. A.; Madala, N. E., Analyses of chlorogenic acids and related cinnamic acid derivatives from Nicotiana tabacum tissues with the aid of UPLC-QTOF-MS/MS based on the in-source collision-induced dissociation method. *Chem. Cent. J.* **2014**, 8, (1), 66-66.
62. Yu, D. Q.; Chen, Y.; Liang, X. T., Structural chemistry and biological activities of natural products from Chinese herbal medicines – *Part II. Res. Commun. Mol. Path.* **2000**, 108, (5-6), 393-436.
63. Wen, L.; You, L.; Yang, X.; Yang, J.; Chen, F.; Jiang, Y.; Yang, B., Identification of phenolics in litchi and evaluation of anticancer cell proliferation activity and intracellular antioxidant activity. *Free Radic. Biol. Med.* **2015**, 84, 171-84.
64. Zhao, W. H.; Gao, L. F.; Gao, W.; Yuan, Y. S.; Gao, C. C.; Cao, L. G.; Hu, Z. Z.; Guo, J. Q.; Zhang, Y. X., Weight-reducing effect of Acer truncatum Bunge may be related to the inhibition of fatty acid synthase. *Nat. Prod. Res.* **2011**, 25, (4), 422-31.
65. Zhao, W. H.; Gao, C. C.; Ma, X. F.; Bai, X. Y.; Zhang, Y. X., The isolation of 1,2,3,4,6-penta-O-galloyl-beta-D-glucose from Acer truncatum Bunge by high-speed counter-current chromatography. *J. Chromatogr. B* **2007**, 850, (1-2), 523-7.

Sample Availability: Not available.